Title

Functional prediction of DNA/RNA-binding proteins by deep learning from gene expression correlations

Naoki Osato [1*]

[1] School of Life Science and Technology, Institute of Science Tokyo, Tokyo, Japan.

E-mail: naokiosato11@gmail.com

*Corresponding author.

Abstract

Deep learning methods have been developed to predict gene expression levels in different cell and tissue types from DNA-binding sites of proteins including transcription factors identified by ChIP-seq assay. However, experimental identification of DNA/RNA-binding sites of proteins and functional characterization of proteins are difficult for some proteins. Gene co-expression correlation has been identified from gene expression data among cells and tissues, and includes the interactions between a DNA/RNA-binding protein and other genes. To predict the functional roles of DNA/RNA-binding proteins based on the interactions between a DNA/RNA-binding protein and other genes, I used the interactions to predict gene expression levels by partially replacing the input data in the deep leaning analysis. The correlation coefficient between actual and predicted gene expression levels increased from 0.70 to 0.80, indicating that gene co-expression data contribute to predict gene expression levels. Some of the functional annotations statistically over-represented in the predicted target genes correspond to the known and associated functions of the DNA/RNA-binding proteins, although the same number of randomly selected genes showed negligible over-representation of functional annotations. Some over-represented functional annotations differed from those identified from all co-expressed genes without using deep learning, suggesting that deep learning selected genes for predicting gene expression levels in cell types from all co-expressed genes. Furthermore, functional annotations that are not registered in a database of functional annotations of genes have been confirmed in published studies. It contributes to predict the functional roles of DNA/RNA-binding proteins.

Keywords

Computational biology, Deep learning, Gene expression, Gene regulation, Protein function prediction

Introduction

Deep learning analysis has improved the accuracy of predicting gene expression levels from the binding sites of DNA/RNA-binding proteins including transcription factors and other regulatory factors (Tasaki, et al., 2020). Transcription factors bind to promoters around transcription start sites (TSSs) and enhancers, which are located far upstream and downstream of genes and TSSs. The method predicts gene expression levels in 53 human tissues based on the experimental and predicted data of binding sites of DNA/RNA-binding proteins and miRNAs in promoter and mRNA-transcribed regions. The correlation coefficient between actual and predicted gene expression levels was 0.82. In my previous study, I modified the method to include the data of DNA-binding proteins bound at open chromatin regions in up to 1 Mbp upstream and downstream regions from TSSs, some of which regions would be associated with enhancers, and removed the binding sites of RNA-binding proteins and miRNAs, the correlation coefficient was 0.70 (Osato and Hamada, 2025).

The binding sites of DNA/RNA-binding proteins are identified by experimental assays such as ChIP-seq and ChIA-pet. These assays require high-quality antibodies of the proteins, but it is difficult to obtain high-quality antibodies for some proteins. For some DNA/RNA-binding proteins, it may be impractical to determine the binding DNA/RNA sequences by experimental analysis with the time, cost, and labor available. Large Language Model (LLM)-based deep learning models, such as Enformer, will

predict DNA sequences that are important for predicting gene expression levels (Avsec, et al., 2021). Massively parallel reporter assays detected the activity of hundreds of thousands of sequences (Agarwal, et al., 2025). However, it would be difficult to identify which DNA/RNA-binding proteins bind to the DNA sequences.

Analysis of gene co-expression correlation between cell and tissue types suggested regulatory interactions among genes, including mRNAs encoding DNA/RNA-binding proteins. Gene expression data by RNA-seq assay and the results of gene co-expression correlation analysis are available in databases (Miller and Bishop, 2021; Obayashi, et al., 2023; Raina, et al., 2023; Yang, et al., 2017; Zhu, et al., 2015). Gene co-expression network analysis has been reported (Lemoine, et al., 2021; Obayashi, et al., 2023; Raina, et al., 2023; Stuart, et al., 2003; Warde-Farley, et al., 2010; Wong, et al., 2018). The correlation of gene expression would be regulated by direct and/or non-direct interactions of molecules. Some of the molecules may be elusive to detect by experimental analysis and difficult to predict by other computational analyses. The correlation of gene expression is potentially associated with regulations that have not been identified.

In this study, to investigate the functional annotations enriched in the putative regulatory target genes of a DNA/RNA-binding protein, I used gene co-expression data to extract the interactions between a DNA/RNA-binding protein and other genes. The DNA-binding sites of about 300 proteins with a low contribution score in my previous deep learning model were replaced with those of other DNA/RNA-binding proteins based on gene co-expression data. Deep learning learned to predict gene expression levels and selected interactions between a DNA-binding site and a gene that contribute to the prediction. The regulatory target genes of a transcription factor include functionally related genes (McLean, et al., 2010). Thus, the functional enrichment of genes is

97 potentially discovered, although the prediction of regulatory target genes may not be
98 precise enough to achieve a research purpose. I compared the overlap between the
99 predicted regulatory target genes of a DNA/RNA-binding proteins and the DNA/RNA-
100 binding sites by experimental assays such as ChIP-seq and eCLIP. Then, I performed
101 functional enrichment analyses of the predicted regulatory target genes of ten DNA/RNA-
102 binding proteins and found that the enriched functional annotations corresponded to the
103 known functional annotations in the UniProt database. Furthermore, I discovered that
104 some functional annotations enriched in the putative regulatory target genes of a
105 DNA/RNA-binding protein were not described in the UniProt database, but were
106 investigated in published papers.

107 These analyses would be useful to identify the functional roles and regulatory target
108 genes of DNA/RNA-binding proteins without using experimental data from protein-
109 binding assays, and are expected to predict the direct and non-direct interactions between
110 DNA/RNA-binding proteins and their regulatory target genes, where some interactions
111 may be difficult to study by experimental analysis. This will contribute to the discovery
112 of novel interactions and functions, and reduce the cost of experimental analysis.

113

114 **Results**

115 To examine the effect of the interaction data of co-expressed genes on the
116 prediction of gene expression levels, among 1,310 DNA-binding proteins in the input
117 data of deep learning, 302 DNA-binding proteins with low contribution scores
118 (DeepLIFT scores) were replaced with the interaction data of co-expressed genes
119 encoding DNA-binding proteins and the mRNAs other than DNA/RNA-binding proteins.
120 The DNA-binding proteins encoded by the co-expressed genes were randomly selected

121 from the gene symbols of DNA-binding proteins in the ENPD database (Tak Leung, et
122 al., 2019), and in the other databases of DNA-binding proteins used for the analysis of
123 DNA-binding motifs. Interestingly, the correlation coefficient between actual and
124 predicted gene expression levels increased from 0.70 to 0.80 in human foreskin fibroblast
125 (HFF) cells using co-expression data (**Fig. 2a, b**). Then, among 1,310 DNA-binding
126 proteins, 325 DNA-binding proteins with low contribution scores were replaced with the
127 interaction data of co-expressed genes encoding RNA-binding proteins and other mRNAs.
128 The RNA-binding proteins encoded by the co-expressed genes were randomly selected
129 from the gene symbols of RNA-binding proteins in the ENPD database. The correlation
130 coefficient increased from 0.70 to 0.81 using co-expression data as well (**Fig. 2c**). These
131 results suggest that the interactions of co-expression of genes contribute to the prediction
132 of gene expression levels.

133 The contribution scores of the input data selected from the gene expression
134 correlations were distributed over a wide range between high and low, but the mean and
135 median of the scores were larger than the original (**Fig. 2d and Supplementary Table**
136 **S1**). I examined the distribution of Spearman's correlations between contribution scores
137 and gene expression levels (log2-TPMs, transcripts per million) (**Supplementary Fig.**
138 **S2**), and plotted example relationships between the contribution scores of a DNA/RNA-
139 binding protein and the expression levels of the regulatory target genes across cell types
140 (**Fig. 2e**). Based on the interactions between co-expressed genes and a DNA/RNA-
141 binding protein, deep learning adjusted the prediction model of gene expression levels in
142 each cell type.

143 To investigate whether the regulatory target genes of a DNA/RNA-binding protein
144 selected based on their contribution scores are associated with the DNA/RNA-binding

145 sites of the protein, I used the DNA-binding sites by ChIP-seq assay and the RNA-binding
146 sites by eCLIP assay around the genes, where a DNA-binding site of the protein by ChIP-
147 seq assay within ±5 kb of TSSs or an RNA-binding site of the protein by eCLIP assay in
148 mRNA-transcribed regions of a gene (ChIP-seq data of 32 DNA-binding proteins in
149 HepG2 cell and eCLIP data of 29 RNA-binding proteins in K562 cell). The genes with a
150 DNA-binding site of the protein or an RNA-binding site of the protein corresponded to
151 high positive or low negative contribution scores of the regulatory target genes of the
152 DNA/RNA-binding protein derived from the deep leaning of gene co-expression data
153 (**Fig. 3 and Supplementary Fig. S1**). The high and low contribution scores would be
154 associated with the regulatory functions of activation and repression of gene expression
155 from the description of the contribution score (DeepLIFT score) on the GitHub webpage
156 of DeepLIFT (Shrikumar, et al., 2017) and a previous study using DeepLIFT (Tasaki, et
157 al., 2020).

158 The transcriptional target genes of a transcription factor include associated
159 functions of genes. Functional enrichment of gene annotations would be useful to predict
160 the function of a transcription factor and to confirm that the transcriptional target genes
161 are not randomly selected. To confirm that the regulatory target genes of a DNA/RNA-
162 binding protein predicted by deep leaning of gene expression correlation included
163 associated functions of genes, I examined the functional enrichments of the regulatory
164 target genes of ten DNA/RNA-binding proteins using Gene Ontology (GO) annotations
165 (Ashburner, et al., 2000; Gene Ontology, et al., 2023). The regulatory target genes of the
166 DNA/RNA-binding proteins included the associated functions of the genes and showed
167 the functional enrichments of GO annotations. However, when the same number of target
168 genes of the DNA/RNA-binding proteins were randomly selected from all genes, the

169 functional enrichments of GO annotations were negligibly observed, indicating that the
170 target genes did not include associated functions of genes (**Fig. 4**). For a more detailed
171 functional enrichment analysis of regulatory target genes of DNA/RNA-binding proteins,
172 I used the statistical overrepresentation test of the gene list analysis of Panther DB
173 (https://pantherdb.org/) (Thomas, et al., 2022). The test uses functional annotation
174 databases such as PANTHER Pathways, Protein Class, GO (Gene Ontology)-Slim, GO,
175 and Reactome Pathways. The functional annotations enriched in putative regulatory
176 target genes of a DNA/RNA-binding protein were compared with those of the
177 DNA/RNA-binding protein obtained from the UniProt database (e.g.
178 https://www.uniprot.org/uniprotkb/Q9Y2L8/entry) (UniProt, 2025). The ten examples of
179 DNA/RNA-binding proteins are shown in **Table 1** and **Supplementary Table S4**. The
180 putative functional annotations of the DNA/RNA-binding proteins correspond to and are
181 associated with those in the UniProt database and publications. Notably, among the ten
182 examples, AKAP8 has cell cycle-related functional annotations such as "GO:0000278
183 mitotic cell cycle" and "GO:0044839 cell cycle G2/M phase transition" in the UniProt
184 database (https://www.uniprot.org/uniprotkb/O43823/entry). In this study, AKAP8 was
185 suggested to be involved in circadian clock systems. By searching Google and the
186 PubMed database, I found the following papers showing that AKAP8 is involved in
187 circadian rhythms: "But the genes, such as NFIL3, AKAP8, and SALL3, highly correlated
188 with known molecular clock genes (CRY1) can be identified as the candidate circadian
189 genes." and "AKAP5 and AKAP8 are both involved in the biosynthesis of the circadian
190 hormone melatonin, which is markedly disturbed in people with ASDs." (Poelmans, et
191 al., 2013; Tan, et al., 2024). These results demonstrate that the method and analysis in this
192 study detected known and novel functional annotations associated with DNA/RNA-

193 binding proteins.

194 The deep learning analysis changed the contribution (i.e., weights in the neural
195 network) of a DNA/RNA-binding protein to the prediction of the expression levels of the
196 regulatory target genes of the DNA/RNA-binding protein during the learning phase. To
197 investigate the effect of learning on the functional enrichment analysis of the target genes,
198 I performed the functional enrichment analysis of all co-expressed genes (*z* score > 2) of
199 the ten DNA/RNA-binding proteins using Panther DB, and compared the functional
200 annotations enriched in all co-expressed genes of a DNA/RNA-binding protein and those
201 of the regulatory target genes of the DNA/RNA-binding protein in the deep learning
202 analysis shown in **Table 2** and **Supplementary Table S5**. Although the number of
203 functional annotations enriched in all co-expressed genes of a DNA/RNA-binding protein
204 increased due to the increase in genes, some functional annotations were only or highly
205 enriched in the regulatory target genes of the DNA/RNA-binding protein after learning.
206 Notably, as in the case of AKAP8 functional annotations, circadian rhythm-related
207 functional annotations were detected only after learning (**Table 2** and annotations
208 highlighted in yellow in the 'S2_AKAP8' tab of **Supplementary Table S4**). As for PKM
209 functional annotations, kinase etc. were identified only after learning (**Table 2** and
210 'S2_PKM' in **Supplementary Table S4**). PKM interacts with ALDOA (Snel, et al., 2000;
211 Szklarczyk, et al., 2023) (STRING database interaction, mouse PKM https://string-
212 db.org/network/10090.ENSMUSP00000034834 ; human PKM also has an interaction
213 with ALDOA in the database), and I found research papers supporting that the functional
214 annotation "aldolase (PC00044)" is associated with PKM involved in glycolysis:
215 "Aldolase A (ALDOA) is an enzyme that plays an important role in glycolysis and
216 gluconeogenesis, which is closely related to tumor metabolism" (Tian, et al., 2022; Zhang,

et al., 2017). These functional annotations were enriched after learning. Thus, they would be involved in the functions in K562 cell where the regulatory target genes of an RNA-binding protein were selected. Circadian clocks and PKM would be associated with human acute myeloid leukemia (AML) cells via glycolysis (Lee, 2021; Puram, et al., 2016; Yang, et al., 2024; Zlacka and Zeman, 2021). These results suggest that combining gene co-expression data with deep learning to predict gene expression levels would reveal the functional associations of DNA/RNA-binding proteins in a cell or tissue type.

Discussion

The expression levels of human genes in cell types have been predicted using deep learning based on the DNA-binding sites of proteins. Here, I applied this method to predict unknown interactions between a DNA/RNA-binding protein and genes based on gene expression correlations between cell types. Gene expression correlations were statistically analyzed using gene expression data from RNA-seq experiments in cell and tissue types. Experimental analysis of DNA/RNA-binding sites by ChIP-seq, eCLIP assays, etc. is more time-consuming, expensive, and laborious than RNA-seq experiments. Experimental analysis of DNA/RNA-binding sites is still difficult for some DNA/RNA-binding proteins. Deep learning analysis of DNA/RNA-binding proteins based on correlations of their expression levels with other genes predicted regulatory target genes of the proteins. Regulatory target genes include associated functions of genes. Enrichment analysis of the functional annotations of the regulatory target genes revealed the functional associations and roles of the DNA/RNA-binding proteins. The predicted functional annotations correspond to the known functional annotations of the proteins. Furthermore, functional annotations not described in a database were also discovered and

241 confirmed in published studies.

242 When comparing DNA-binding sites predicted based on the contribution scores for
243 predicting gene expression levels with DNA-binding sites by ChIP-seq assay, the two
244 types of DNA-binding sites may not overlap completely. Although tens of thousands of
245 DNA-binding sites of proteins are identified by ChIP-seq assay, some of them may not
246 be directly involved in the regulation of gene expression. Some transcription factors are
247 involved in multiple functions (Kim, et al., 2015; Ladomery, 1997). The number of co-
248 expressed genes of a DNA/RNA-binding protein with z score > 2 was about less than
249 1,500, and was less than the number of genes with ChIP-seq peaks of the DNA/RNA-
250 binding proteins, but the most of the co-expressed genes with a statistical significance
251 would be involved in the regulation of gene expression. Our previous analysis of
252 insulator-associated DNA-binding proteins revealed that 97 transcription factors and
253 DNA-binding proteins would be associated with insulator functions that affect enhancer-
254 promoter interactions (Osato and Hamada, 2025). Some of them would be important for
255 the formation of chromatin loops, transcriptional condensates and/or phase separation,
256 which are different mechanisms to affect gene expression from the direct regulation of
257 genes by transcription factors. In the deep learning analysis of insulator-associated DNA-
258 binding proteins, we used eQTL data to find DNA-binding sites of proteins that affect
259 gene expression levels. However, in this study, I did not use the DNA-binding motif
260 sequences of proteins and open chromatin regions by DNase-seq or ATAC-seq assay to
261 identify their DNA-binding sites because the purpose of this study is to investigate DNA-
262 binding proteins whose DNA-binding motifs are unknown. Moreover, the association
263 between eSNP and eGene of eQTL data may include indirect interactions. The
264 contribution scores of DNA-binding sites of proteins selected based on gene expression

correlation showed higher or lower scores, suggesting that indirect interactions between DNA-binding proteins and other genes would affect the scores.

As for the analysis of functional enrichment of regulatory target genes of a DNA-binding protein, ten DNA/RNA-binding proteins correspond to the known functional annotations of the DNA/RNA-binding proteins, suggesting that the number of predicted regulatory target genes is sufficient to identify the functional annotations of the proteins by a statistical test. The identification of functional enrichments of regulatory target genes of a protein seemed to require more than one hundred of genes by a Fisher's exact test adjusted with a false discovery rate (FDR) in Panther DB. The number of regulatory target genes of some proteins was less than a hundred, and their functional enrichments seemed to be difficult to identify. One of the next steps of this study would be to improve the method for identifying the functional enrichments of a small number of genes by considering other information such as gene expression levels and correlation of gene expression.

When I replaced all the input data of the deep learning analysis with the interactions between DNA/RNA-binding proteins and other genes based on gene expression correlation, the number of functional enrichments of predicted regulatory target genes of a DNA/RNA-binding protein was reduced, and the result of the functional enrichment analysis did not include the same functional annotations as the known functional annotations of the DNA/RNA-binding protein in the UniProt database. Thus, the high replacement ratio of the input data would lead to learning error-prone interactions between a DNA/RNA-binding protein and regulatory target genes. In my previous study, when the regulatory target genes of a DNA-binding protein were replaced by randomly selected genes, the number of functional enrichments decreased as the number of

randomly selected genes increased. The number of functional enrichments normalized to the total number of genes reflects the accuracy of the regulatory target genes (Osato, 2018).

The DNA-binding proteins were ranked according to the contribution scores of their DNA-binding sites for each gene. When the rank of a DNA-binding protein is higher or equal to 50 or lower or equal to 1,260 out of a total of 1,310, the functional enrichments of putative target genes appeared to be identified by the statistical test in Panther DB. Some DNA/RNA-binding proteins did not have high or low-ranking putative regulatory target genes in HepG2 cells. These proteins may have high or low-ranking target genes in other cell types, and thus functional enrichment analysis of target genes could be performed to reveal their functional roles. Some transcription factors and DNA-binding proteins would bind to each other to form the protein complex and regulate gene expression levels (Burley and Kamada, 2002)(Goos, et al., 2022)(Berenson, et al., 2023). These proteins would bind to the same promoters of genes and the ranking of each protein in the complex may not always be high or low. Analysis of the co-localization of DNA/RNA-binding proteins would reveal the functional roles of the protein complex.

The deep learning model, model parameters, and analysis methods used in this study could be adapted and improved for the purpose of this study. I examined a small number of DNA/RNA-binding proteins in a few cell types in this study, and would be able to predict the functional roles of a larger number of DNA/RNA-binding proteins in cell and tissue types. The results of the analysis would be useful to understand and study the biological and molecular functions of unknown functions of DNA/RNA-binding proteins and their regulatory target genes.

313 # Methods

314 **Deep learning analysis**

315 I modified the deep learning method for predicting gene expression levels among
316 cell and tissue types based on the DNA-binding sites of transcription factors and other
317 regulators, and included the DNA-binding sites of transcription factors in regions far
318 upstream and downstream of TSSs (Osato and Hamada, 2025; Tasaki, et al., 2020) (**Fig.**
319 **1**). To reduce the heterogeneity of cells in a tissue, I used gene expression data of cell
320 types. The gene expression data of different cell types were obtained from public
321 databases: human foreskin fibroblasts (HFFs) (GSM941744), human mammary epithelial
322 cells (HMECs) (Encyclopedia of DNA Elements at UCSC
323 http://genome.ucsc.edu/encode/,
324 'wgEncodeCshlLongRnaSeqHmecCellPapAlnRep1.bam') (Barrett, et al., 2013; Edgar, et
325 al., 2002), neural progenitor cells (NPCs) (GSM915326, ENCFF529SIO), human
326 hepatoma cell line (HepG2) (ENCFF670LIE), and human leukemia cell line (K562)
327 (ENCFF584WML). FPKM values of gene expression levels were calculated based on
328 GENCODE V19 gene annotations in the ENCODE portal database
329 (https://www.encodeporoject.org/) (Luo, et al., 2020; Mudge, et al., 2025) using the
330 RSeQC tool (http://rseqc.sourceforge.net/) (Wang, et al., 2012). The FPKM values were
331 transformed to log2-fold with the addition of 0.25 to avoid negative infinity results. Log2-
332 fold changes relative to the median log2-FPKM across the four cell types were calculated
333 according to the original deep learning method (transcriptome data processing as
334 described by Tasaki et al.) (Osato and Hamada, 2025; Tasaki, et al., 2020).

335 The DNA-binding sites overlapping with open chromatin regions in putative
336 enhancers located outside of promoter regions were added as input data in the deep

337 learning method. To identify the DNA-binding sites of DNA-binding proteins (DBPs) in
338 promoter and enhancer regions, ChIP-seq data of the DBPs were obtained from GTRD
339 database release v20.06 (https://gtrd.biouml.org) (Kolmykov, et al., 2021). The binding
340 site of a DBP that regulates the expression level of each transcript was selected based on
341 eQTL data (GTEx_Analysis_v8_eQTL.tar) from GTEx portal release v8
342 (https://gtexportal.org). The DNA-binding site located within a 100-bp region around a
343 single-nucleotide polymorphism (SNP) of an eQTL was supposed to regulate the
344 expression of the transcript corresponding to the eQTL. I did not use *trans*-eQTL data,
345 where the SNP of an eQTL was not located on the same chromosome as the transcribed
346 region of the eQTL. The genomic locations of the eQTLs were converted to the
347 corresponding locations in the hg19 version of the human genome using the LiftOver tool
348 (http://hgdownload.soe.ucsc.edu/downloads.html#liftover) (Hinrichs, et al., 2006).

349 The original model of the input data of DNA-binding sites in promoter regions was
350 used for the deep learning analysis: the lengths of a DBP ChIP-seq peak in each 100-base
351 bin in a region between 2 kbp upstream and 1 kbp downstream of the TSS of each gene
352 or transcript (**Fig. 1**). To add the input data of DNA-binding sites of DBPs in more
353 upstream and downstream regions of a TSS and reduce the number of bins, I first
354 computed the length of a DBP ChIP-seq peak in a 100-base bin and then selected the
355 maximum length in each interval of 100 bins in a region between 1 megabase upstream
356 and downstream of a TSS. This step outputted the maximum 200 longest DBP ChIP-seq
357 peaks for each transcript. I modified the original model and extended it to include the
358 data.

359 In the training of the modified deep learning model, I used the same test, training,
360 and validation data as in the original method: all 2,705 genes encoded on chromosome 1

361 as test data, training data (22,251 genes), and validation data (2,472 genes) randomly
362 selected from the other genes (Osato and Hamada, 2025; Tasaki, et al., 2020). The
363 DeepLIFT tool was used to calculate the contribution scores of DNA-binding sites of
364 proteins, which are important for predicting gene expression levels (Shrikumar, et al.,
365 2017). The input data for promoters and putative enhancer regions were concatenated into
366 a total of 230 bins of the lengths of 1,310 DBP ChIP-seq peaks, consisting of 30 bins for
367 promoters and 200 bins for putative enhancers, because the DeepLIFT tool 'RevealCancel
368 rule on dense layers and the Rescale rule on conv layers (genomics default)', with high
369 scoring accuracy, cannot be applied to a neural network with multiple input layers.
370 Ubuntu (version 20.04), Python (version 3.8.10), TensorFlow (version 2.6.0), NVIDIA
371 CUDA toolkit (version 11.4.2), GeForce RTX 3080 GPU with 10 GB memory, and Intel
372 Core i7-10700 CPU with 128 GB memory were used for training and prediction, and the
373 original scripts were modified to run on newer versions of the software. The training
374 method was the same as the original, and the training time was two to four hours.
375
376 **Functional prediction of DNA/RNA-binding proteins**
377 To predict the regulatory target genes of DNA/RNA-binding proteins without using
378 data from protein binding assays such as ChIP-seq or eCLIP, among 1,310 DNA-binding
379 proteins in the input data of deep learning, 302 DNA-binding proteins with lower
380 contribution scores for predicting gene expression levels were replaced by other DNA-
381 binding proteins. For the analysis of RNA-binding proteins, 325 DNA-binding proteins
382 were replaced by RNA-binding proteins. The gene symbols of RNA-binding proteins
383 were obtained from the ENPD database (Tak Leung, et al., 2019). The interactions
384 between replaced DNA/RNA-binding proteins and genes regulated by the proteins were

385 estimated based on the co-expression pairs of genes between cells and tissues obtained
386 from the COEXPRESdb (Obayashi, et al., 2023). Gene co-expression is the similarity of
387 expression profiles between a pair of genes. Functionally related genes and genes with
388 the same regulation are generally expressed together between cell and tissue types. If a
389 gene encoding a DNA/RNA-binding protein shows a similar expression pattern with
390 other genes, they are potentially regulated by the protein and functionally related. The co-
391 expression interactions with z score > 2 between the genes encoding other DNA/RNA-
392 binding proteins and the genes other than DNA/RNA-binding proteins were used as input
393 data, replacing those with lower contribution scores. The binding sites of the DNA- and
394 RNA-binding protein were hypothetically located at 2 kb upstream of the TSSs and TSSs
395 of the co-expressed genes, respectively. Deep learning and the DeepLIFT tool with the
396 new input data calculated the contribution scores of the binding sites of DNA/RNA-
397 binding proteins for predicting gene expression levels.

398 For each DNA/RNA-binding protein, I examined the rank of the contribution score
399 of the DNA/RNA-binding site by comparing it with the contribution scores of the other
400 DNA/RNA-binding proteins for each gene. According to the tendency of high or low
401 ranks (i.e., high positive or low negative contribution scores) of DNA/RNA-binding sites
402 of a protein among its regulatory target genes, I selected regulatory target genes with high
403 or low ranks, where the rank within the top five or bottom five for each gene, of
404 DNA/RNA-binding sites of the protein as the primary target genes regulated by the
405 protein. The rank threshold for selecting primary target genes was adjusted for each
406 DNA/RNA-binding protein to detect functional enrichments. To obtain functional
407 enrichments associated with the DNA/RNA-binding protein, the rank threshold was
408 restricted within the top five or bottom five, except for RPLP0, within the top eight to

409 increase the number of genes. The functional enrichment analysis of the primary target
410 genes regulated by the DNA/RNA-binding protein was performed using in-house scripts
411 and the 'Statistical overrepresentation test' of Panther DB (https://pantherdb.org/)
412 (Thomas, et al., 2022). Using in-house scripts to perform functional enrichment analyses
413 of different gene sets, I compared the number of functional enrichments of Gene Ontology
414 (GO) annotations among the primary target genes of a DNA/RNA-binding protein, all co-
415 expressed genes (z score > 2), and randomly selected genes with the same number of the
416 co-expressed genes. GO annotations from three organizations: biological process,
417 molecular function, and cellular component were merged. The GO file
418 (https://purl.obolibrary.org/obo/go.obo) file and the human gene annotation file
419 (https://current.geneontology.org/annotations/goa_human.gaf.gz) were downloaded from
420 the gene ontology resource (https://geneontology.org/docs/download-ontology/)
421 (Ashburner, et al., 2000; Gene Ontology, et al., 2023). The HUGO Gene Nomenclature
422 Committee (HGNC) database was used to transform human gene symbols to Ensemble
423 Gene IDs (https://www.genenames.org/). For Panther DB analysis, the Ensemble Gene
424 IDs of the primary target genes were used as the analyzed gene set, and the Ensemble
425 Gene IDs in the gene expression data for deep leaning were used as the reference gene
426 set. Fisher's exact test was performed with adjustment for the Benjamini-Hochberg false
427 discovery rate.

428 To examine the binding sites of ChIP-seq data and eCLIP data around the
429 regulatory target genes of DNA/RNA-binding proteins predicted by deep learning of gene
430 co-expression data, I selected the DNA-binding sites within ±5 kbp of a TSS of a gene by
431 ChIP-seq assay or the RNA-binding sites between the transcription start and end of a gene
432 by eCLIP assay based on the Human GENCODE v19 gene annotation (Mudge, et al.,

433 2025). For this analysis, ChIP-seq data of 32 DNA-binding proteins and eCLIP data of
434 29 RNA-binding proteins were obtained from the ENCODE portal and the paper
435 (**Supplementary Table S6**) (Van Nostrand, et al., 2020). I also examined the ratios of the
436 number of genes with high and low contribution scores of the DNA/RNA-binding site
437 around genes with the DNA/RNA-binding site by ChIP-seq or eCLIP assays.
438

439 ## Figures

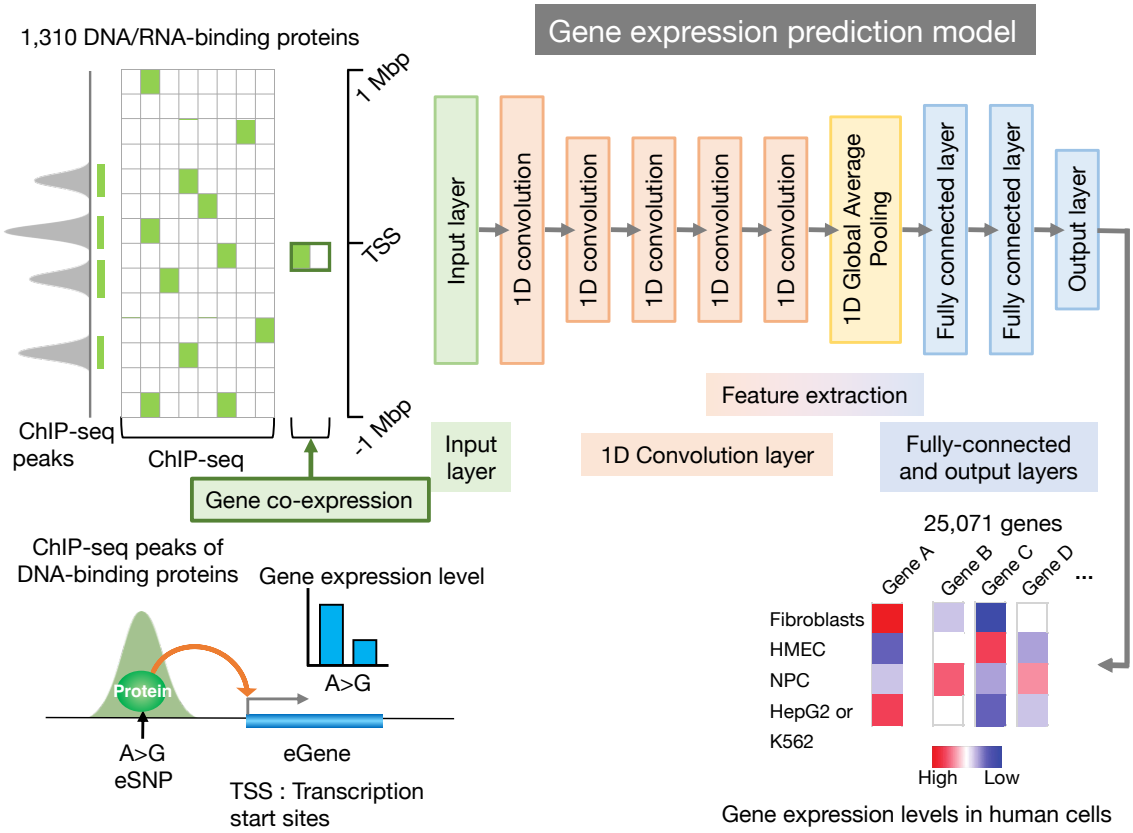

440

441 **Figure 1. Overview of prediction of gene expression levels.** The output data of gene
442 expression levels in human cells were predicted from the input data of genomic locations
443 of DNA-binding sites of proteins at promoters and more distant regions. In the machine
444 learning phase, a DNA-binding protein bound to a distant region overlapping an eSNP
445 was associated with a gene (eGene) that was potentially regulated by the DNA-binding

446 protein based on the eSNP and eGene of the eQTL data. Based on the association of each
447 gene, the locations of ChIP-seq peaks of DNA-binding proteins were binned (green box)
448 and summarized in a matrix as input data.
449

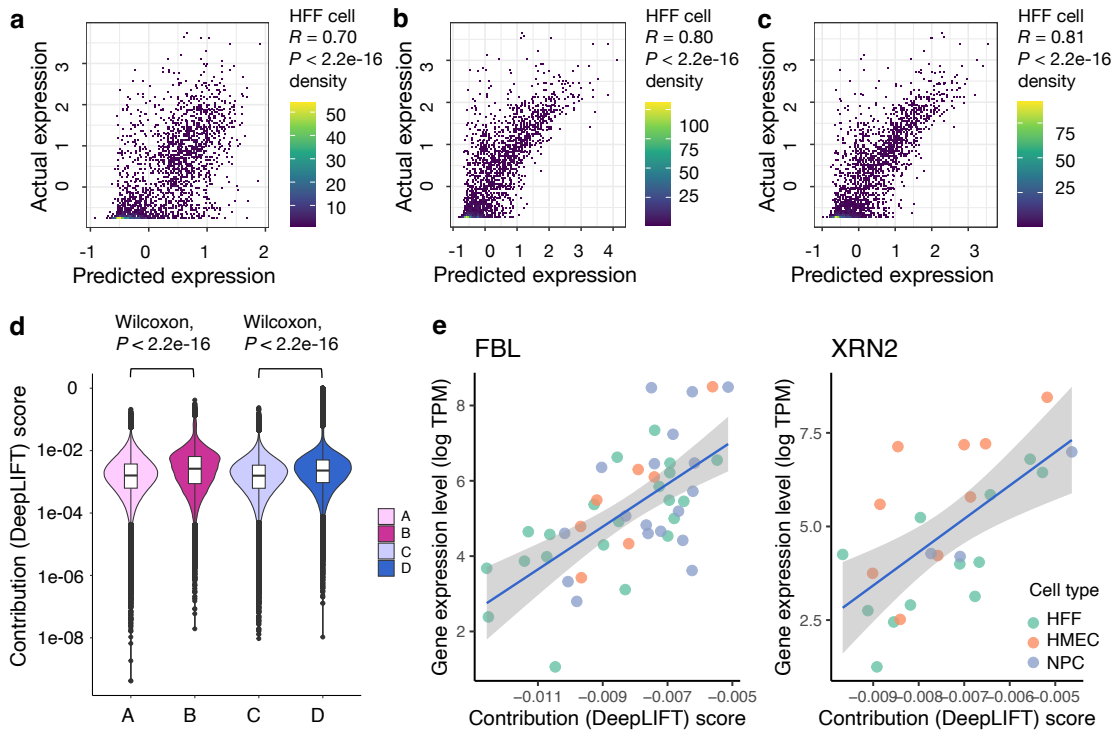

450

451 **Figure 2. Comparison of actual and predicted gene expression levels.**
452 The predicted log2-TPM (transcripts per million) values of genes were compared with
453 the actual expression levels in HFF cells using Spearman's rank correlation. **a** The input
454 data for deep learning consists of the DNA-binding sites of 1,310 DNA-binding proteins
455 from ChIP-seq data. **b** Among 1,310 proteins, 302 DNA-binding proteins with low
456 contribution scores were replaced by the same number of DNA-binding proteins selected
457 based on gene expression correlation data. **c** Among 1,310 proteins, 325 DNA-binding
458 proteins with low contribution scores were replaced by the same number of RNA-binding
459 proteins selected based on gene expression correlation data. **d** DNA-binding sites based

on co-expression data showed higher contribution (DeepLIFT) scores. A and C: Binding sites of DNA-binding proteins were obtained from ChIP-seq data. B and D: Binding sites based on co-expression data between genes. A and B: Positive contribution scores. C and D: Absolute values of negative contribution scores. (Wilcoxon signed-rank test, $P < 2.2e-16$) **e** Example relationships between the predictive contributions of a regulator and its expression levels across tissues. A line of best fit based on linear regression was depicted with 95 percent confidence intervals.

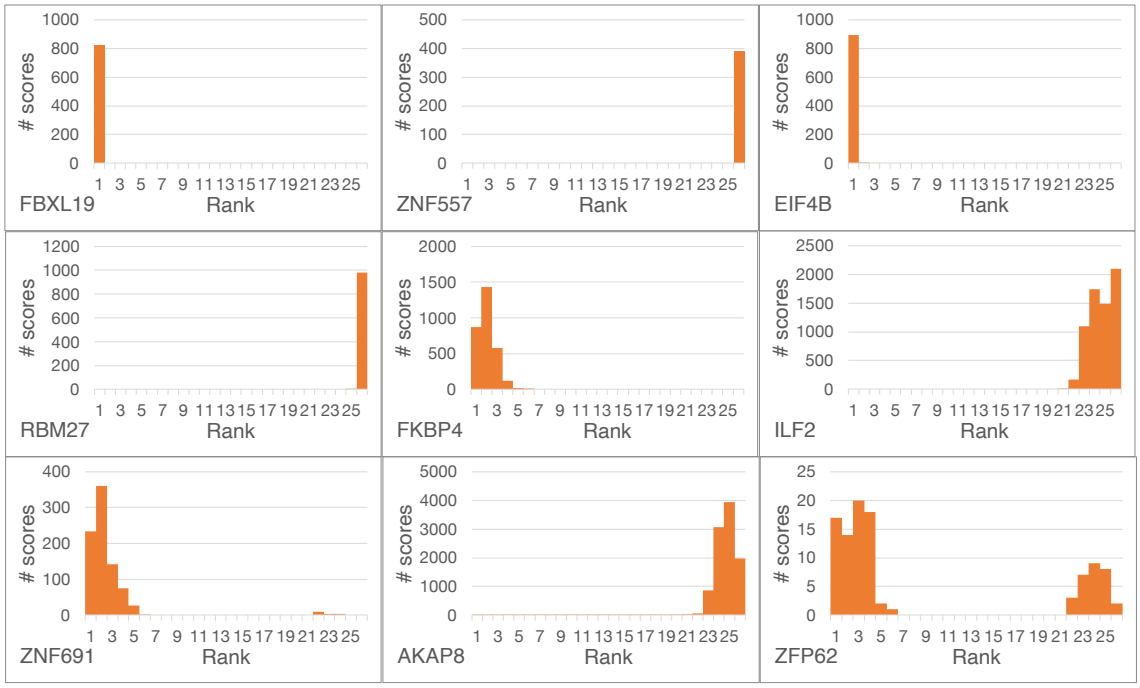

Figure 3. Comparison of predicted target genes with experimental data. The *x* axis shows the rank of the contribution score of a DNA/RNA-binding site for predicting a gene expression level. Contribution scores of DNA/RNA-binding sites were ranked from 1 (high positive contribution scores, left end) to 1,310 (low negative contribution scores, right end), binned with fifty rank intervals. Rank 1 on the *x* axis represents 1 to 50 ranks, rank 2 represents 51 to 100 ranks, and the last rank 26 represents 1,251 to 1,310 ranks.

475 The DNA/RNA-binding sites were hypothetically located in promoters or genes bound
476 by the DNA/RNA-binding protein of each graph. The DNA/RNA-binding sites located
477 in promoters or genes bound by the DNA/RNA-binding protein show higher or lower
478 contribution scores than the DNA-binding sites of the ChIP-seq data as a whole. The *y*
479 axis shows the number of contribution scores in each bin of fifty rank intervals. Positive
480 contribution scores would correspond to activation and negative scores would correspond
481 to repression of gene expression.
482

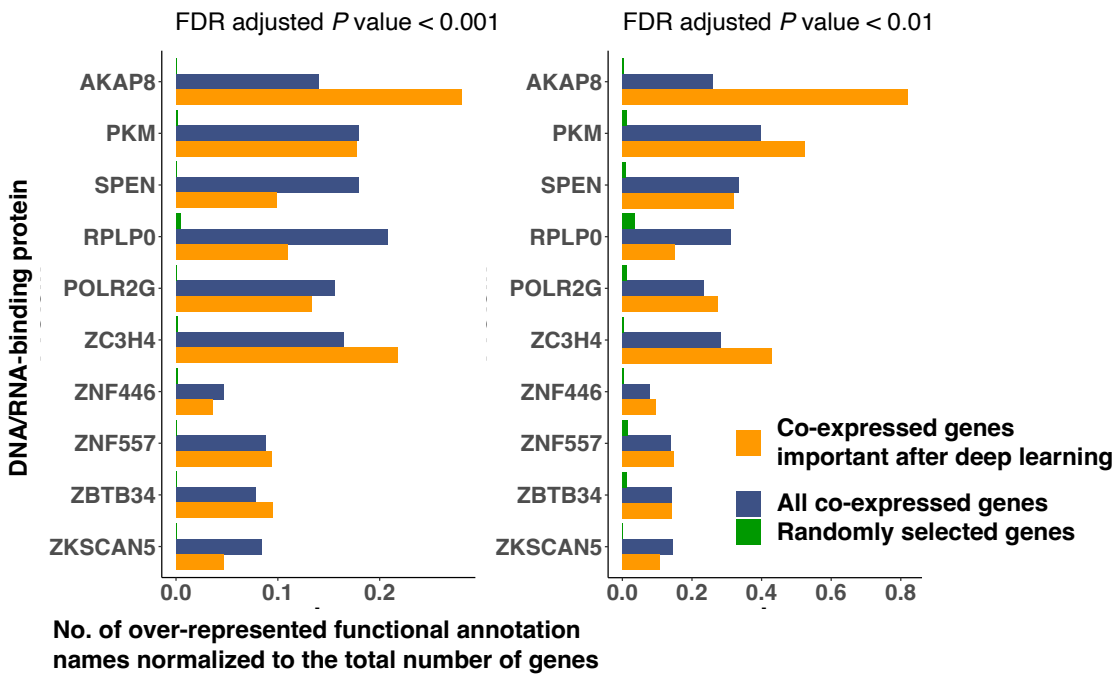

483

484 **Figure 4. Number of functional annotation names over-represented in the target**
485 **genes of a DNA/RNA-binding protein.**

486 The regulatory target genes of a DNA/RNA-binding protein include associated functions
487 of genes. The functional enrichment analysis was performed on co-expressed genes that
488 contributed to the prediction of gene expression levels in the deep leaning analysis, all
489 co-expressed genes with *z* score > 2, and randomly selected genes with the same total

490 number as all co-expressed genes. The gene ontology functional annotations in the three
491 categories such as biological process, molecular function and cellular component were
492 merged and used for the enrichment analysis. The *P* values of Fisher's exact test were
493 adjusted by the false discovery rate (FDR).
494
495
496 ## Tables
497 **Table 1. Common functional annotations between a DNA/RNA-binding protein and**
498 **its putative regulatory target genes.**
499 The functional annotations of DNA/RNA-binding proteins were obtained from the
500 UniProt database. The functional annotations statistically enriched in their putative
501 regulatory target genes were derived from Panther DB. Gray lines separate each
502 annotation.
503

ZKSCAN5
DNA-binding transcription factor activity
C2H2 zinc finger transcription factor
RNA polymerase II cis-regulatory region sequence-specific DNA binding
metal ion binding
ZBTB34
C2H2 zinc finger transcription factor
DNA-binding transcription activator activity, RNA polymerase II-specific
RNA polymerase II transcription regulatory region sequence-specific DNA binding
ZNF557
DNA-binding transcription activator activity, RNA polymerase II-specific
RNA polymerase II transcription regulatory region sequence-specific DNA binding
ion binding, metal ion binding
ZNF446
C2H2 zinc finger transcription factor
extracellular space
ZC3H4
chromatin/chromatin-binding, or -regulatory protein
transcription regulator activity
metal ion binding
POLR2G
RNA polymerase II transcription regulatory region sequence-specific DNA binding
general transcription factor
translational protein
RPLP0
large ribosomal subunit
ribonucleoprotein complex
cytosolic large ribosomal subunit
SPEN
mRNA binding
chromatin binding
transcription coregulator activity
PKM
kinase
glycolytic process
ATP metabolic process
AKAP8
negative regulation of RNA biosynthetic process
Circadian clock system
Cry-Per complex

Table 2. Functional enrichments detected in the regulatory target genes of an RNA-binding protein.

The functional enrichment analysis was performed by Panther DB. The table shows the functional annotations statistically enriched in the regulatory target genes of an RNA-binding protein after deep learning based on co-expressed genes, but not statistically enriched in all the co-expressed genes (*z* score > 2) including the RNA-binding protein. 'Reference' is the number of human genes, 'Analyzed' is the number of human regulatory target genes of an RNA-binding protein, 'Expected' is the number of genes with the

514 functional annotation (e.g. Circadian clock system) estimated from the ratio of genes with
515 the functional annotation in the reference genes, 'Over/Under' stands for
516 overrepresentation and underrepresentation, 'Fold Enrichment' is the ratio of the number
517 of analyzed genes with the functional annotation to the expected number of genes, 'raw
518 P-value' is the P-value of Fisher's exact test, and FDR is the Benjamini-Hochberg false
519 discovery rate of the test.

520

AKAP8							
PANTHER Pathways							
PANTHER Pathways	Reference (17130)	Analyzed (49)	Expected	Over/ Under	Fold Enrichment	raw P-value	FDR
Circadian clock system (P00015)	10	3	0.03	+	> 100	2.60E-06	4.16E-04
PANTHER GO-Slim Biological Process							
PANTHER GO-Slim Biological Process	Reference (17130)	Analyzed (49)	Expected	Over/ Under	Fold Enrichment	raw P-value	FDR
circadian regulation of gene expression (GO:0032922)	16	3	0.05	+	65.55	1.20E-05	1.27E-02
response to light stimulus (GO:0009416)	21	3	0.06	+	49.94	2.82E-05	1.99E-02
circadian rhythm (GO:0007623)	21	3	0.06	+	49.94	2.82E-05	1.49E-02
rhythmic process (GO:0048511)	24	3	0.07	+	43.7	4.27E-05	1.81E-02
GO cellular component complete							
GO cellular component complete	Reference (17130)	Analyzed (49)	Expected	Over/ Under	Fold Enrichment	raw P-value	FDR
Cry-Per complex (GO:1990512)	3	2	0.01	+	> 100	2.40E-05	4.77E-02
PKM							
PANTHER Protein Class							
PANTHER Protein Class	Reference (17130)	Analyzed (326)	Expected	Over/ Under	Fold Enrichment	raw P-value	FDR
aldolase (PC00044)	5	2	0.1	+	21.02	3.48E-03	5.68E-02
kinase (PC00137)	134	9	2.55	+	3.53	1.07E-03	2.62E-02
PANTHER GO-Slim Molecular Function							
PANTHER GO-Slim Molecular Function	Reference (17130)	Analyzed (326)	Expected	Over/ Under	Fold Enrichment	raw P-value	FDR
enzyme inhibitor activity (GO:0004857)	107	8	2.04	+	3.93	1.01E-03	4.68E-02
kinase activity (GO:0016301)	562	23	10.7	+	2.15	7.08E-04	3.57E-02
PANTHER GO-Slim Biological Process							
PANTHER GO-Slim Biological Process	Reference (17130)	Analyzed (326)	Expected	Over/ Under	Fold Enrichment	raw P-value	FDR
endoplasmic reticulum tubular network organization (GO:0071786)	12	3	0.23	+	13.14	1.32E-03	3.68E-02
regulation of cellular component biogenesis (GO:0044087)	139	10	2.65	+	3.78	3.31E-04	1.05E-02

521

522

Acknowledgements

Supercomputing resources were provided by the Human Genome Center of the Institute of Medical Science at the University of Tokyo and ROIS National Institute of Genetics.

Author contributions

N.O. designed and performed the research, and wrote and revised the manuscript.

Supplementary data

Supplementary data are available at

Conflict of interests

None declared.

Funding

This work was supported by the Japan Society for the Promotion of Science (JSPS) KAKENHI [16K00387], Osaka University start-up research grant, KIOXIA young scientist research grant at Waseda University; and Sumitomo basic science research projects to NO.

Data availability

Human foreskin fibroblast (HFF) cell RNA-seq data were obtained from GSM941744 in the Gene Expression Omnibus (GEO) database. The RNA-seq data of human mammary epithelial cells (HMEC) were found on ENCODE at UCSC

547 http://genome.ucsc.edu/encode/ at
548 'wgEncodeCshlLongRnaSeqHmecCellPapAlnRep1.bam'. Human neural progenitor cell
549 (NPC) RNA-seq data were obtained from GSM915326. HepG2 and K562 RNA-seq data
550 were obtained from ENCFF670LIE.bam and ENCFF584WML.bam in the ENCODE
551 portal (https://www.encodeproject.org/). Co-expression data of mRNAs were
552 downloaded from COXPRESdb (https://zenodo.org/record/6861444/files/Hsa-u.v22-
553 05.G16651-S245698.combat_pca.subagging.z.d.zip). The list of DNA/RNA-binding
554 proteins were obtained from ENPD database (http://qinlab.sls.cuhk.edu.hk/ENPD/).
555 ChIP-seq data of TFs were downloaded from the v20.06 release of the GTRD database
556 (https://gtrd.biouml.org). eQTL data (GTEx_Analysis_v8_eQTL.tar) were downloaded
557 from the v8 release of the GTEx portal (https://gtexportal.org). eCLIP data of RNA-
558 binding proteins were obtained from ENCSR456FVU in the ENCODE portal and from
559 Supplementary Data 2 in the paper (Van Nostrand EL et al. *Nature* 2020 doi:
560 10.1038/s41586-020-2077-3).
561
562
563 **References**
564
565 Agarwal, V., *et al.* Massively parallel characterization of transcriptional regulatory elements.
566 *Nature* 2025.
567 Ashburner, M., *et al.* Gene ontology: tool for the unification of biology. The Gene Ontology
568 Consortium. *Nature genetics* 2000;25(1):25-29.
569 Avsec, Z., *et al.* Effective gene expression prediction from sequence by integrating long-range
570 interactions. *Nature methods* 2021;18(10):1196-1203.
571 Barrett, T., *et al.* NCBI GEO: archive for functional genomics data sets--update. *Nucleic acids*
572 *research* 2013;41(Database issue):D991-995.
573 Berenson, A., *et al.* Paired yeast one-hybrid assays to detect DNA-binding cooperativity and

574 antagonism across transcription factors. *Nat Commun* 2023;14(1):6570.
575 Burley, S.K. and Kamada, K. Transcription factor complexes. *Curr Opin Struct Biol*
576 2002;12(2):225-230.
577 Edgar, R., Domrachev, M. and Lash, A.E. Gene Expression Omnibus: NCBI gene expression and
578 hybridization array data repository. *Nucleic acids research* 2002;30(1):207-210.
579 Gene Ontology, C.*, et al.* The Gene Ontology knowledgebase in 2023. *Genetics* 2023;224(1).
580 Goos, H.*, et al.* Human transcription factor protein interaction networks. *Nat Commun*
581 2022;13(1):766.
582 Hinrichs, A.S.*, et al.* The UCSC Genome Browser Database: update 2006. *Nucleic acids research*
583 2006;34(Database issue):D590-598.
584 Kim, S., Yu, N.K. and Kaang, B.K. CTCF as a multifunctional protein in genome regulation and
585 gene expression. *Exp Mol Med* 2015;47(6):e166.
586 Kolmykov, S.*, et al.* GTRD: an integrated view of transcription regulation. *Nucleic acids research*
587 2021;49(D1):D104-D111.
588 Ladomery, M. Multifunctional proteins suggest connections between transcriptional and post-
589 transcriptional processes. *Bioessays* 1997;19(10):903-909.
590 Lee, Y. Roles of circadian clocks in cancer pathogenesis and treatment. *Exp Mol Med*
591 2021;53(10):1529-1538.
592 Lemoine, G.G.*, et al.* GWENA: gene co-expression networks analysis and extended modules
593 characterization in a single Bioconductor package. *BMC Bioinformatics* 2021;22(1):267.
594 Luo, Y.*, et al.* New developments on the Encyclopedia of DNA Elements (ENCODE) data portal.
595 *Nucleic acids research* 2020;48(D1):D882-D889.
596 McLean, C.Y.*, et al.* GREAT improves functional interpretation of cis-regulatory regions. *Nature*
597 *biotechnology* 2010;28(5):495-501.
598 Miller, H.E. and Bishop, A.J.R. Correlation AnalyzeR: functional predictions from gene co-
599 expression correlations. *BMC Bioinformatics* 2021;22(1):206.
600 Mudge, J.M.*, et al.* GENCODE 2025: reference gene annotation for human and mouse. *Nucleic*
601 *acids research* 2025;53(D1):D966-D975.
602 Obayashi, T.*, et al.* COXPRESdb v8: an animal gene coexpression database navigating from a
603 global view to detailed investigations. *Nucleic acids research* 2023;51(D1):D80-D87.
604 Osato, N. Characteristics of functional enrichment and gene expression level of human putative
605 transcriptional target genes. *BMC Genomics* 2018;19(Suppl 1):957.
606 Osato, N. and Hamada, M. Systematic discovery of directional regulatory motifs associated with
607 human insulator sites. *bioRxiv* 2025.
608 Poelmans, G.*, et al.* AKAPs integrate genetic findings for autism spectrum disorders. *Transl*
609 *Psychiatry* 2013;3(6):e270.

610 Puram, R.V., *et al.* Core Circadian Clock Genes Regulate Leukemia Stem Cells in AML. *Cell*
611 2016;165(2):303-316.
612 Raina, P., *et al.* GeneFriends: gene co-expression databases and tools for humans and model
613 organisms. *Nucleic acids research* 2023;51(D1):D145-D158.
614 Shrikumar, A., Greenside, P. and Kundaje, A. Learning Important Features Through Propagating
615 Activation Differences. In: Doina, P. and Yee Whye, T., editors, *Proceedings of the 34th*
616 *International Conference on Machine Learning*. Proceedings of Machine Learning Research:
617 PMLR; 2017. p. 3145--3153.
618 Snel, B., *et al.* STRING: a web-server to retrieve and display the repeatedly occurring
619 neighbourhood of a gene. *Nucleic acids research* 2000;28(18):3442-3444.
620 Stuart, J.M., *et al.* A gene-coexpression network for global discovery of conserved genetic modules.
621 *Science (New York, N.Y.)* 2003;302(5643):249-255.
622 Szklarczyk, D., *et al.* The STRING database in 2023: protein-protein association networks and
623 functional enrichment analyses for any sequenced genome of interest. *Nucleic acids research*
624 2023;51(D1):D638-D646.
625 Tak Leung, R.W., *et al.* ENPD - A Database of Eukaryotic Nucleic Acid Binding Proteins: Linking
626 Gene Regulations to Proteins. *Nucleic acids research* 2019;47(D1):D322-D329.
627 Tan, X., *et al.* Novel Insights into the Circadian Rhythms Based on Long Noncoding and Circular
628 RNA Profiling. *Int J Mol Sci* 2024;25(2).
629 Tasaki, S., *et al.* Deep learning decodes the principles of differential gene expression. *Nat Mach*
630 *Intell* 2020;2(7):376-386.
631 Thomas, P.D., *et al.* PANTHER: Making genome-scale phylogenetics accessible to all. *Protein Sci*
632 2022;31(1):8-22.
633 Tian, W., *et al.* Bioinformatics analysis of the role of aldolase A in tumor prognosis and immunity.
634 *Sci Rep* 2022;12(1):11632.
635 UniProt, C. UniProt: the Universal Protein Knowledgebase in 2025. *Nucleic acids research*
636 2025;53(D1):D609-D617.
637 Van Nostrand, E.L., *et al.* A large-scale binding and functional map of human RNA-binding
638 proteins. *Nature* 2020;583(7818):711-719.
639 Wang, L., Wang, S. and Li, W. RSeQC: quality control of RNA-seq experiments. *Bioinformatics*
640 *(Oxford, England)* 2012;28(16):2184-2185.
641 Warde-Farley, D., *et al.* The GeneMANIA prediction server: biological network integration for
642 gene prioritization and predicting gene function. *Nucleic acids research* 2010;38(Web Server
643 issue):W214-220.
644 Wong, A.K., Krishnan, A. and Troyanskaya, O.G. GIANT 2.0: genome-scale integrated analysis of
645 gene networks in tissues. *Nucleic acids research* 2018;46(W1):W65-W70.

646 Yang, S., *et al.* COEXPEDIA: exploring biomedical hypotheses via co-expressions associated with
647 medical subject headings (MeSH). *Nucleic acids research* 2017;45(D1):D389-D396.
648 Yang, Y., Pu, J. and Yang, Y. Glycolysis and chemoresistance in acute myeloid leukemia. *Heliyon*
649 2024;10(15):e35721.
650 Zhang, F., *et al.* Elevated transcriptional levels of aldolase A (ALDOA) associates with cell cycle-
651 related genes in patients with NSCLC and several solid tumors. *BioData Min* 2017;10:6.
652 Zhu, Q., *et al.* Targeted exploration and analysis of large cross-platform human transcriptomic
653 compendia. *Nature methods* 2015;12(3):211-214, 213 p following 214.
654 Zlacka, J. and Zeman, M. Glycolysis under Circadian Control. *Int J Mol Sci* 2021;22(24).

655